BONDED CONTACT PROBLEM FOR AN ELASTIC LAYER UNDER TENSION

Mehmet Ruşen Geçit*

Mechanical Engineering Department,
King Fahd University of Petroleum & Minerals,
Dhahran 31261, Saudi Arabia

الخلاصـــة :

يهتم هذا البحث بدراسة مشكلة الانفعال المستوي لصفيحة مرنة مربوطة بقاعدة صلبة . تطبق قوة شد الى الأعلى على السطح العلوي للصفيحة عبر شريحة صلبة لها سماكة محدودة . وأدى التحليل للصفيحة غير القابلة للانضغاط الى ايجاد نظام مكّون من معادلتين تكامليتين مفردتين من النوع الأول للأجهاد العمودي على السطح البيني والاجهاد القصي على قاعدة الشريحة الصلبة . ويتم حل هاتين المعادلتين التكامليتين رقمياً . وتمّ حساب توزيعات معاملات الاجهاد لأشكال هندسية متعددة .

ABSTRACT

This paper considers the plane strain problem of an elastic layer bonded to a rigid foundation. An upward tensile force is applied to the top surface of the layer through a rigid strip of finite thickness. The analysis for the incompressible layer leads to a system of two singular integral equations of the first kind for the interface normal and shear stresses at the base of the rigid strip. These integral equations are solved numerically, and the stress distributions and stress intensity factors are calculated for various geometries.

*Address for correspondence :
KFUPM Box No. 840
King Fahd University of Petroleum & Minerals
Dhahran 31261
Saudi Arabia.

BONDED CONTACT PROBLEM FOR AN ELASTIC LAYER UNDER TENSION

1. INTRODUCTION

Almost every engineering design requires connections between several components. A serious disadvantage of mechanical connectors, such as screws, rivets, or welding, is that they do not distribute the load uniformly and hence result in large local stresses. This problem can sometimes be overcome by joining the components with use of adhesives. One of the major difficulties associated with adhesives is the determination of their strength characteristics. Many standard test methods have been developed on adhesives (see, for example, reference [1]). However, predicting performance of the bond in actual applications is not straightforward using a strength of materials approach with these standard tests. The principles of fracture mechanics can be employed for this purpose. Often new tests or modifications of existing tests are required to obtain the related fracture mechanics properties.

Consider a linearly elastic isotropic and incompressible layer bonded to a rigid foundation along its entire bottom surface (Figure 1). The layer is under the action of an upward force applied through a rigid strip bonded to its top surface. The problem under consideration may represent a typical pull-off test geometry for adhesives, the elastic layer being the adhesive to be tested and rigid strip being, for example, a relatively rigid metal plate attached to it.

2. FORMULATION OF THE PROBLEM

Consider the elastostatic plane strain problem for a layer shown in Figure 1. Layer material is linearly elastic isotropic and incompressible. The effect of the gravitation is neglected. The layer of thickness h is perfectly bonded to a rigid foundation along its entire bottom surface and to a rigid strip of thickness $2a$ on its top surface through while a tensile force $P=2ap_0$ is applied. Due to symmetry about $x=0$ plane, it is sufficient to consider the problem in $x \geq 0$ only. Under these circumstances, the governing equations of the plane elasticity must be solved subject to the following boundary conditions

$$u(x,0)=0\,, \quad v(x,0)=0\,, \quad (0 \leq x < \infty)\,, \tag{1a, b}$$

$$u(x,h)=0\,, \quad v(x,h)=v_0\,, \quad (0 \leq x < a)\,,$$
$$\tau_{xy}(x,h)=0\,, \quad \sigma_y(x,h)=0\,, \quad (a < x < \infty)\,, \tag{2a-d}$$

where u and v are the x and y components of the displacement vector and the constant v_0 can be determined from the equilibrium condition

$$\int_0^a \sigma_y(x,h)\,dx = \frac{P}{2}\,, \tag{3}$$

Solution of the governing equations can be obtained using, for example, the classical Fourier transform method which yields the expressions (see, for example, [2, 3])

$$u = \frac{2}{\pi}\int_0^\infty [(A+ryB)\,e^{-ry} + (C+ryD)\,e^{ry}]\sin(rx)\,dr\,,$$

$$v = \frac{2}{\pi}\int_0^\infty \{[A+(1+ry)B]\,e^{-ry} - [C-(1-ry)D]\,e^{ry}\}\cos(rx)\,dr\,, \tag{4a, b}$$

$$\tau_{xy} = \frac{4\mu}{\pi}\int_0^\infty r[-(A+ryB)e^{-ry} + (C+ryD)e^{ry}]\sin(rx)dr,$$

$$\sigma_y = \frac{4\mu}{\pi}\int_0^\infty r\{-[A+(1+ry)B]e^{-ry} - [C-(1-ry)D]e^{ry}\}\cos(rx)\,dr\,, \tag{5a, b}$$

where μ is the shear modulus. The unknowns $A-D$ are to be determined from the boundary conditions at $y=0$ and $y=h$. The mixed conditions (2) can be written more appropriately in the form

$$\frac{\partial}{\partial x}u(x,h)=0, \qquad \frac{\partial}{\partial x}v(x,h)=0, \qquad (0 \leq x < a)\,, \tag{6a, b}$$

$$\sigma_y(x,h)=p_1(x)\,, \quad \tau_{xy}(x,h)=p_2(x)\,, \quad (0 \leq x < \infty)\,, \tag{7a, b}$$

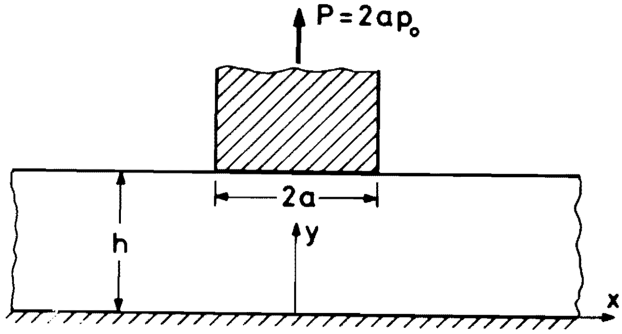

Figure 1. Elastic Layer Bonded to a Rigid Foundation.

such that

$$p_1(x) = p_2(x) = 0, \qquad (a < x < \infty) , \qquad (8a, b)$$

by introducing two new unknown function p_1 and p_2, the interface normal and shear stresses. Now, substituting Equations (4) and (5) into conditions (1) and (7), $A-D$ can be expressed in terms of p_1 and p_2 as

$$A = -C = rh(e^{-rh}+e^{rh})P_1 - [(1+rh)e^{-rh}+(1-rh)e^{rh}]P_2 ,$$

$$B = -[e^{-rh}+(1+2rh)\, e^{rh}]\, P_1 + [e^{-rh}+(1-2rh)\, e^{rh}]\, P_2 ,$$

$$D = [(1-2rh)\, e^{-rh}+e^{rh}]\, P_1 + [(1+2rh)\, e^{-rh}+e^{rh}]\, P_2 , \qquad (9a-d)$$

$$P_1 = \frac{1}{2\mu r\Delta}\int_0^a p_1(t)\cos(rt)\, dt ,$$

$$P_2 = \frac{1}{2\mu r\Delta}\int_0^a p_2(t)\sin(rt)\, dt ,$$

$$\Delta = e^{2rh}+2+4r^2h^2+e^{-2rh} \qquad (10a-c)$$

so that the stresses and the displacements are all expressed in terms of p_1 and p_2.

3. THE INTEGRAL EQUATIONS

The two unknown functions p_1 and p_2 are determined by using the conditions (6) which result in the following system of singular integral equations

$$\sum_{n=1}^{2}\frac{1}{\pi}\int_{-a}^{a}\left[\frac{\delta_{mn}}{t-x}+k_{mn}(x,\, t)\right]p_n(t)\, dt = 0 ,$$

$$(-a < x < a) , \quad (m = 1, 2) , \qquad (11a, b)$$

where δ_{mn} is the Kronecker delta and the Fredholm kernels $k_{mn}(x, t)$ are given by

$$k_{mn}(x,\, t) = \int_0^\infty K_{mn}(x,\, t,\, r)\, \Delta^{-1}\, dr , \quad (m,\, n = 1, 2) ,$$

$$K_{11} = -[2+4rh+4r^2h^2-4r^2h^2\, e^{-2rh}-e^{-4rh}]\sin(t-x)\, r,$$

$$K_{12} = [4r^2h^2+2(1+2r^2h^2)\, e^{-2rh}+e^{-4rh}]\cos(t-x)\, r ,$$

$$K_{21} = [1-4r^2h^2-2(1+2r^2h^2)\, e^{-2rh}-e^{-4rh}]\cos(t-x)\, r,$$

$$K_{22} = [-2+4rh-4r^2h^2+4r^2h^2 e^{-2rh}+e^{-4rh}]\sin(t-x)\, r. \qquad (12a-h)$$

The system of singular integral equations (11) must be solved subject to the equilibrium conditions

$$\int_{-a}^{a} p_n(t)\, dt = \delta_{1n}\, P, \quad (n = 1, 2). \qquad (13a, b)$$

In order to simplify the numerical analysis, introduce the following dimensionless variables

$$w = x/a , \qquad s = t/a. \qquad (14a, b)$$

Then, Equations (11) and (13) may be rewritten as

$$\sum_{n=1}^{2}\frac{1}{\pi}\int_{-1}^{1}\left[\frac{\delta_{mn}}{s-w}+ak_{mn}(aw,\, as)\right]p_n(as)\, ds = 0 ,$$

$$(-1 < w < 1) , \qquad (m = 1, 2) .$$

$$\int_{-1}^{1} p_m(as)\, ds = 2\delta_{1m}p_0 , \qquad (15a-d)$$

Due to the singular term $(s-w)^{-1}$, the solution will be sought in terms of sectionally holomorphic functions [4]. The unknown functions p_1 and p_2 are singular at $w = \pm 1$ [1, 5, 6]. This singular behavior may be determined by writing

$$p_n(aw) = g_n(w)\, (1-w^2)^{-\lambda}\, p_0 ,$$

$$(0 < Re(\lambda) < 1) , \qquad (n = 1, 2) , \quad (16a, b)$$

where g_1 and g_2 are Hölder-continuous functions in $[-1, 1]$, and by examining the singular integral equations (15a, b) near the end points $w = \pm 1$. Following the complex function technique outlined in [4] one can write

$$p_n(aw) = \frac{g_n(-1)p_0}{2^\lambda(1+w)^\lambda} + \frac{g_n(1)p_0}{2^\lambda(1-w)^\lambda} + O(1), \ (n = 1, 2) , \qquad (17a, b)$$

as $w \to \pm 1$ so that

$$\frac{1}{\pi}\int_{-1}^{1}\frac{p_n(as)}{s-w}ds = \frac{g_n(-1)p_0\cot\pi\lambda}{2^\lambda(1+w)^\lambda}$$

$$-\frac{g_n(1)p_0\cot\pi\lambda}{2^\lambda(1-w)^\lambda} + O(1), \ (n = 1, 2) , \qquad (18a, b)$$

as $w \to \pm 1$. Then, with use of Equations (18) and the fact that $g_n(\pm 1) \neq 0$, $(n = 1, 2)$, one can continue in a similar way as described in [7] and obtain the result[1]

$$\lambda = 0.5. \qquad (19)$$

This value is in agreement with the previously reported results (see, for example, [5, 6, 8]). Having determined λ, one can use the Gauss integration formula [10] and reduce Equations (15) to the following system of algebraic equations

[1]If the layer were compressible, $\lambda = 0.5 \pm (i/2\pi)\ln(3-4\nu)$ where ν is the Poisson's ratio. In that case, the numerical scheme would be entirely different (see [9]), which is beyond the scope of this paper.

$$\sum_{i=1}^{N} \sum_{n=1}^{2} C_i \left[\frac{\delta_{mn}}{s_i - w_j} + a k_{mn}(a w_j, a s_i) \right] g_n(s_i) = 0,$$

$$(j = 1, \ldots, N-1), \qquad (m = 1, 2),$$

$$\sum_{i=1}^{N} C_i \, g_m(s_i) = 2\delta_{1m}/\pi \, , \qquad (20)$$

where

$$C_1 = C_N = \frac{1}{2(N-1)}, \quad C_i = \frac{1}{N-1}(i=2,\ldots,N-1) \, ,$$

$$s_i = \cos\left(\frac{i-1}{N-1}\pi\right), \qquad (i = 1,\ldots,N) \, ,$$

$$w_j = \cos\left(\frac{j-1}{2N-2}\pi\right), \qquad (j = 1,\ldots,N-1) \, . \qquad (21)$$

4. NUMERICAL RESULTS

Some of the calculated results are shown in Figures 2–9. Figures 2 and 3 show the variations of the normalized stresses p_1/p_0 and p_2/p_0 (see Equations (7)) over the normalized interval $x/a < 1$ along the rigid strip–layer interface for various a/h ratios. Note that for a fixed uniform stress p_0 and a fixed layer thickness, the resultant force P decreases with decreasing a/h ratio. The case $a/h = 0.01$ may represent that of a concentrated force directly applied to the layer. As can be observed from these figures, stress distributions depend heavily on a/h ratio. As a/h decreases, p_1 decreases over the central portion whereas it increases near the edges. On the other hand, p_2 decreases with decreasing a/h ratio in general. One must be aware of the fact that under the action of the upward force, the points on the top surface of the layer will have a tendency to move towards the centre $x = 0$. But, this tendency is restricted along the interface by the shear stresses resulting from the bonded contact with the rigid strip. As the thickness of the rigid strip decreases, size of the restricted region becomes smaller and consequently the required shear stresses for restriction of horizontal displacement will be smaller. Both normal and shear stresses tend to infinity as the end point $x = a$ is reached. Stress state in the close vicinity of the corners of the rigid strip can be described in terms of the stress intensity factors defined by

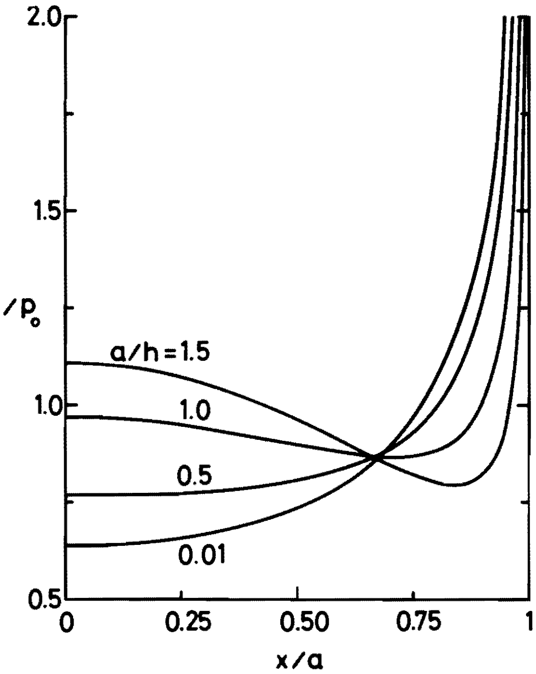

Figure 2. Normal Stress between the Layer and the Rigid Strip.

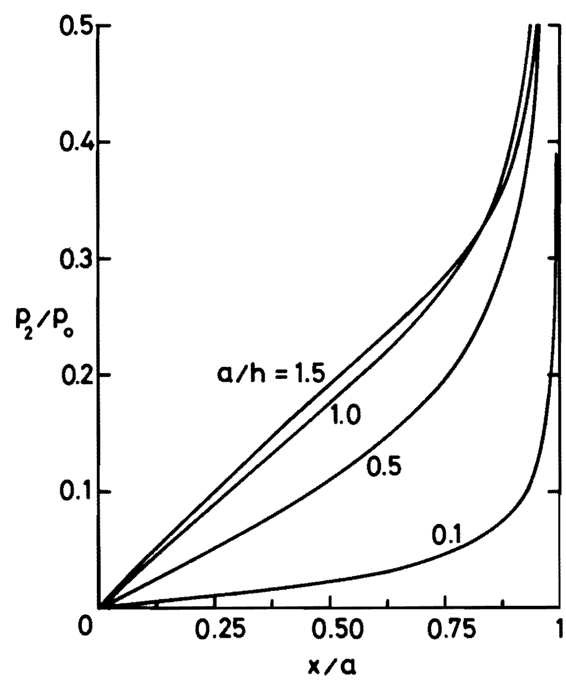

Figure 3. Shear Stress between the Layer and the Rigid Strip.

$$k_1 = \lim_{x \to a} [2(a-x)]^{1/2} \, \sigma_y(x, h) \, ,$$

$$k_2 = \lim_{x \to a} [2(a-x)]^{1/2} \, \tau_{xy}(x, h) \, . \qquad (22a, b)$$

Figure 4 shows the variations of the normalized stress intensity factors

$$\bar{k}_n = k_n / p_0 \, a^{1/2} \, , \qquad (n = 1, 2) \, , \qquad (23a, b)$$

with a/h. As a/h approaches zero, the constraint on

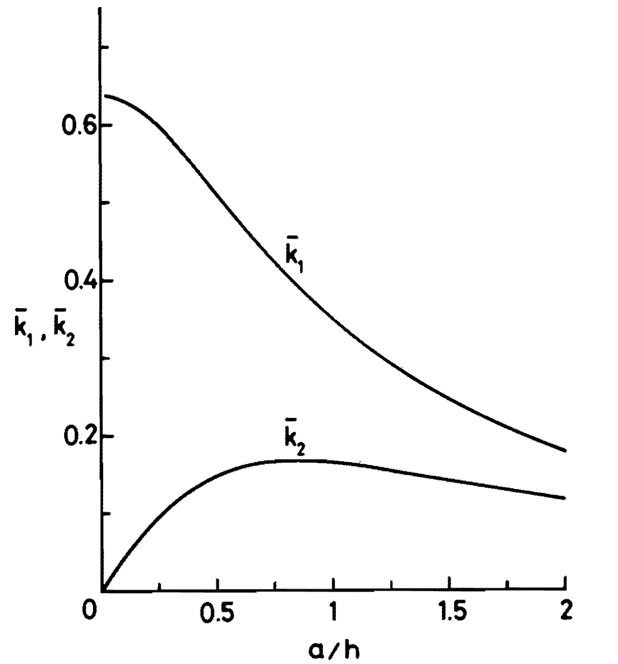

Figure 4. Stress Intensity Factors at the Corners of the Rigid Strip.

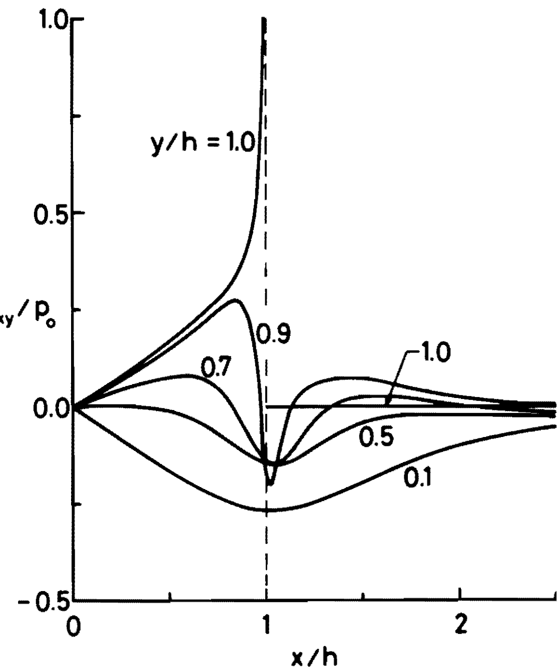

Figure 6. Shear Stress Distributions When a = h.

the top surface of the layer due to the rigid strip regarding the horizontal displacement simply disappears and the shear component of the stress intensity factor, $\bar{k}_2$, vanishes.

Figures 5 and 6 show the normal and shear stress distributions, respectively, at several levels in the layer when $a = h$. Distributions are smoother at low levels and they possess significant variations as the level under consideration gets closer to the top surface, the most extensive disturbance being realized around $x = a$. Figures 7 and 8 show the stress distributions at a level of $y = 0.7h$ for several a/h ratios. These stresses are normalized using

$$\sigma_0 = P/2h = (a/h)\, p_0 \tag{24}$$

so that the resultant force P can be kept constant while a/h varies which may provide a better understanding in comparing results for several a/h ratios. For a fixed force P, the normal stress acting through the rigid strip–layer interface becomes more concentrated when a/h decreases. Consequently, one may expect more disturbed distributions in the layer for smaller a/h ratios. This trend can be well observed in Figures 7 and 8. As a/h increases the stress distributions become smoother.

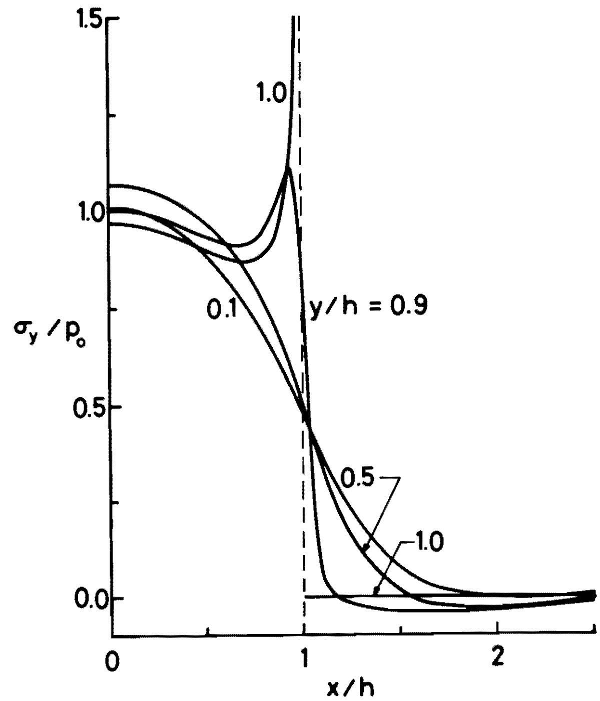

Figure 5. Normal Stress Distributions When a = h.

Finally, Figure 9 shows the contours of equal maximum shear stress τ_{max}/p_0 when $a = h$. One may note the accumulation of the contours around $x = a$, $y = h$. As expected, the maximum shear stress is quite insignificant when $x > a$.

It must be pointed out that the results given in this paper for the tensile layer can be used for the compressive layer problem as well. If the tensile

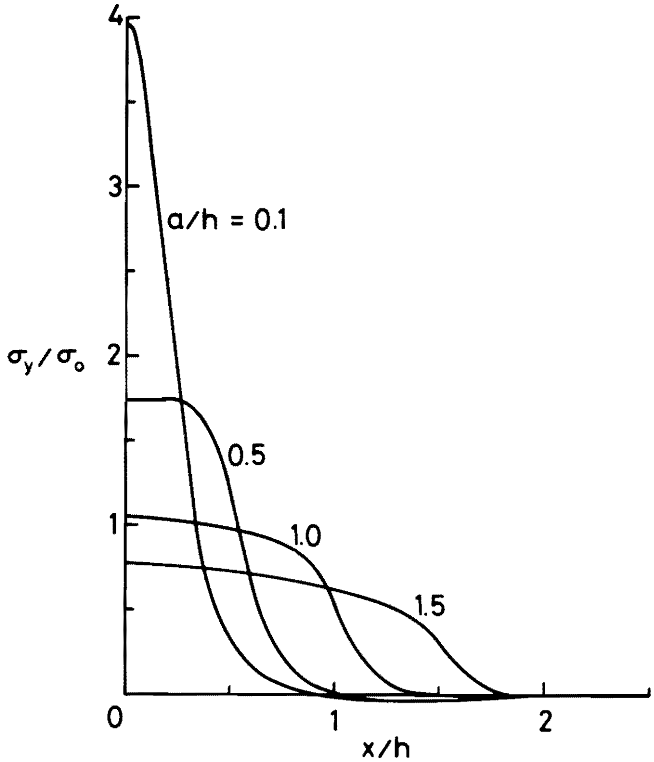

Figure 7. Normal Stress Distributions at y = 0.7 h.

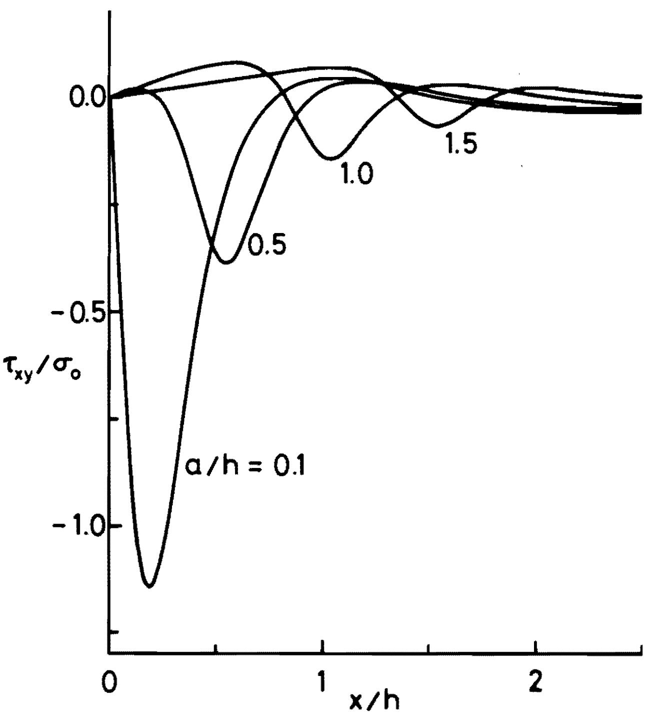

Figure 8. Shear Stress Distributions at y = 0.7 h.

force is replaced by a compressive one, Figures 2–8 will give the stress distributions provided the sign is reversed and Figure 9 will remain unchanged.

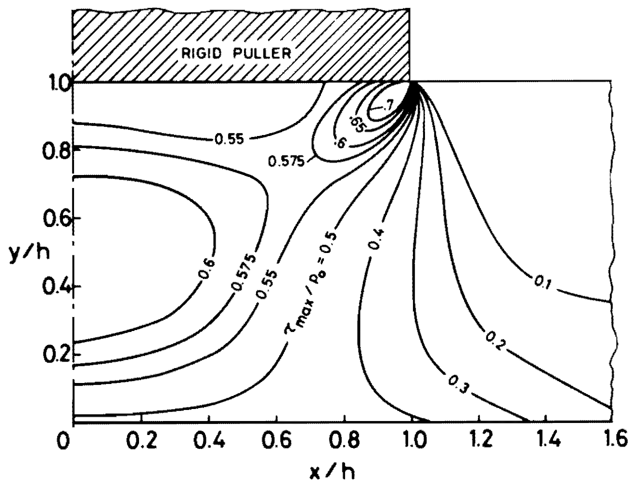

Figure 9. Maximum Shear Stress Contours When a = h.

REFERENCES

[1] G. P. Anderson, S. J. Bennett, and K. L. DeVries, *Analysis and Testing of Adhesive Bonds*. New York: Academic Press, 1977.

[2] M. R. Geçit, "A Tensionless Contact without Friction between an Elastic Layer and an Elastic Foundation", *International Journal of Solids and Structures,* **16** (1980), p. 387.

[3] M. R. Geçit and S. Gökpinar, "Frictionless Contact between an Elastic Layer and a Rigid Rounded Support", *Arabian Journal for Science and Engineering,* **10** (1985), p. 243.

[4] N. I. Muskhelishvili, *Singular Integral Equations*. Gröningen: P. Noordhoff, 1953.

[5] G. G. Adams and D. B. Bogy, "The Plane Solution for the Elastic Contact Problem of a Semi-Infinite Strip and Half Space", *ASME Journal of Applied Mechanics,* **43** (1976), p. 603.

[6] G. G. Adams, "A Semi-Infinite Elastic Strip Bonded to an Infinite Strip", *ASME Journal of Applied Mechanics,* **47** (1980), p. 789.

[7] T. S. Cook and F. Erdogan, "Stresses in Bonded Materials with a Crack Perpendicular to the Interface", *International Journal of Engineering Science,* **10** (1972), p. 677.

[8] D. B. Bogy, "Two Edge-Bonded Elastic Wedges of Different Materials and Wedge Angles under Surface Tractions", *ASME Journal of Applied Mechanics,* **38** (1971), p. 377.

[9] F. Erdogan, "Approximate Solutions of Systems of Singular Integral Equations", *SIAM Journal of Applied Mathematics,* **17** (1969), p. 1041.

[10] S. Krenk, "Quadrature Formulae of Closed Type for Solution of Singular Integral Equations", *Journal of the Institute of Mathematics and Its Applications,* **22** (1978), p. 99.

Paper Received 17 November 1985; Revised 16 March 1986.